J Comp Physiol A (2004) 190: 365–377
DOI 10.1007/s00359-004-0502-y

ORIGINAL PAPER

W. D. Chapple · J. L. Krans

Cuticular receptor activation of postural motoneurons in the abdomen of the hermit crab, *Pagurus pollicarus*

Received: 30 July 2003 / Revised: 8 January 2004 / Accepted: 21 January 2004 / Published online: 20 February 2004

Abstract Displacement of the abdominal cuticle of the hermit crab, *Pagurus pollicarus*, activates motoneurons of the ventral superficial muscles that mediate posture and slow movements. Five excitatory motoneurons innervating the right ventral superficial muscle of the fourth abdominal segment were activated in a phasic stereotyped fashion in the isolated nervous system. Intracellular records from these motoneurons showed an initial monosynaptic burst, a period of inhibition in which inhibitory post-synaptic potentials were present and then a later period of increased spike frequency generated by excitatory post-synaptic potentials. The reflex response was maintained after severing all ganglionic roots from peripheral structures, isolating the nerve cord from peripheral feedback pathways. The two excitatory components of the response showed a dependence on strain that was much smaller than that found in sensory afferents. There was no relationship between the site of touch to the cuticle and the intensity or pattern of activation of the motoneurons. The reflex burst produced a transient activation of both longitudinal and transverse/circular layers of the muscle with forces that varied between 10% and 25% of the maximum muscle force. These results are consistent with a feedforward regulation of muscle stiffness.

Keywords Arthropod · Crustacean · Feedforward Open-loop · Reflex

Abbreviations DSM: dorsal superficial muscle · ejp: excitatory junction potential · EMG: electromyogram · epsp: excitatory post-synaptic potential · ipsp: inhibitory post-synaptic potential · PSDF: probability spike density function · PSTH: peristimulus time histogram · VSM: ventral superficial muscle

W. D. Chapple (✉) · J. L. Krans
Department of Physiology and Neurobiology,
University of Connecticut, Storrs, CT 06269, USA
E-mail: chapple@predator.pnb.uconn.edu
Tel.: +1-860-4864558

Introduction

Hermit crabs are decapod Crustacea that live in gastropod shells. Shell support is a specialized postural task that is controlled by motor centers in both the thorax and abdomen. An analysis of how this control is achieved may provide insight into more general mechanisms of postural control. Although postural control has been studied for many years in many animals, there has been an increasing recognition over the last two decades that this control is complex. For example, a lateral push to the torso of a dog first elicits a reflex stiffening of the contralateral legs, but as the displacement is continued, lateral steps or hops are executed (Roberts 1967). Three mechanisms (Houk and Rymer 1981; Duysens et al. 2000) are operating: (1) the reflex stiffening of the legs by stretch reflexes, (2) the mechanical properties of tonically activated muscle, and (3) a switch to a different motor pattern. The active mechanical properties of muscle can act rapidly so that they can potentially compensate for some disturbances without requiring central nervous system intervention. These properties are part of a broad range of mechanical adaptations that animals use to simplify and reduce the energy requirements of posture and movement (Full and Koditschek 1999; Dickinson et al. 2000). How animals combine these mechanical properties with central nervous system processes is clearly important for our understanding of motor control.

There are a number of examples of reflexes that appear to exploit these mechanical properties, often by feedforward mechanisms. For example, the monosynaptic component of the stretch reflex in mammals compensates for short-range yield in muscle by a rapid recruitment of additional motor units in response to stretch (Nichols and Houk 1976; Cordo and Rymer 1982). Maintenance of limb position involves co-contraction of antagonist muscles around a joint as well as reciprocal innervation (Feldman 1980). This co-con-

traction stiffens the joint and assists it in resisting disturbances. The control of joint stiffness is a complex process that must blend the reciprocal innervation of muscle with co-contraction and involves contributions from a variety of mechanoreceptors (Prochazka 1996; Nichols et al. 1999). In addition, perturbation of stance is also controlled by visual and vestibular pathways (Horak and MacPherson 1996), so that central nervous system circuitry must combine this information to exploit muscle properties.

A number of lines of evidence suggest that hermit crabs exploit the active properties of muscle in regulating shell posture. Using still photography and electromyogram (EMG) recordings it was observed that hermit crabs support their shells at heights above the substrate that varied with shell weight (Chapple 1973a, 1973b). EMG recordings of abdominal ventral superficial muscle (VSM) motoneurons in these animals showed variations in motoneuron frequency during behavior as well as an increase in motoneuron firing frequency with greater loads. However, when weights were applied only to the abdomen in intact animals, no relationship was observed between static load and motoneuron firing frequency; reflex activation of the motoneurons was entirely phasic. This suggested that muscle tone was not generated by length signals from the abdomen. When the 4th and 5th walking legs, which together with the abdomen support and stabilize the shell, were removed the animal could support the weight of a light plastic shell with the abdomen alone; if the motor nerves of the 3rd and 4th abdominal ganglia were destroyed, with the walking legs intact, animals could carry light plastic shells in an abnormal position only for short periods of time. These results indicated that the abdomen was an important component of the shell support system and appeared to behave as a curved cantilever, with the VSM opposing the weight of the shell. Stretch of the VSM in isolated abdomen preparations in which both sensory and motor nerves were intact showed the same pattern of reflex activation of the muscles as in intact animals (Chapple 1985). Reflex stretch transiently doubled muscle stiffness, but the stiffness did not vary significantly with stretch amplitude, velocity or the initial length of the VSM. Static changes in length of the VSM, either in the intact animal or in the isolated abdomen, did not alter tonic motoneuron firing frequency that did maintain muscle stiffness at levels higher than in passive muscle. In contrast, sinusoidal or 'pink noise' variations in muscle length showed an initial elevation in motoneuron firing frequency and muscle stiffness after which there was an adaptation to a 'steady-state' level significantly above the tonic frequency of the motoneurons (Chapple 1997). As in the ramp stretch measurements of muscle stiffness, 'pink noise' stimulation doubled stiffness but had no effect on the time constants of the muscle. The VSM is composed of an inner layer of longitudinal fibers and two additional layers of muscle fibers oriented in a circular and transverse orientation. Reflex activation by mechanoreceptors co-activates all of these layers as well as the reduced superficial dorsal muscles (DSM), thus increasing the hydrostatic pressure of the soft abdomen as well as its stiffness. Since the VSM are slow muscles the latency for their activation is sufficiently long that it is unlikely that they could compensate for rapid disturbances.

It was initially believed that the mechanoreceptors that reflexly activate the motoneurons were transducing muscle force. However, a recent examination of their properties (Chapple 2002) showed that their threshold to muscle stretch is higher than to external displacement of the cuticle, that they have wide receptive fields with considerable overlap among receptors, that their maximum sensitivity is not to the cuticle above the postural muscle but to an adjacent region that contacts the shell, and that above a low-frequency region of the spectrum they signal cuticular displacement with a pronounced adaptation of their response. This raised the question of how the motoneurons are reflexly activated; do they vary muscle force over a wide or a narrow range? Are the different components of the reflex response produced primarily by peripheral mechanisms or is there a substantial central component as well? Is there evidence for a differential activation of VSM motoneurons by stimuli to different regions of the abdominal surface?

The present experiments examine the response of the VSM motoneurons to mechanical activation of mechanoreceptors and electrical stimulation of their axons in the right 1st root of the 4th abdominal ganglion. These two methods of stimulation elicit a complex pattern of motoneuron activation that persists in the isolated ganglion. Intracellular recordings from the motoneurons provide evidence for the involvement of both excitatory and inhibitory interneurons in the response. Motoneuron firing frequency does not vary greatly with stimulus intensity nor does the reflex force produced by the muscle. We interpret these results to suggest that the reflex produces a fast relatively stereotyped activation of the muscle to a plateau level of stiffness that is then maintained by the later portion of the reflex, and that the reflex is a feedforward mechanism for increasing active muscle stiffness.

Materials and methods

Specimens of *Pagurus pollicarus* were collected from sublittoral protected areas in Fishers Island Sound off the coast of Connecticut. The posterior abdomen was exposed with a longitudinal incision along its medial dorsal surface, the hepatopancreas removed, and the abdominal nervous system was exposed by removing the large fast flexor muscles of the third, fourth and fifth segments. Our nomenclature for identifying nerves was described in

Chapple (1997)[1], Briefly, the abdominal segment is specified, followed by the side (r, right; l, left), and the number of the root of the ganglion; thus, 4r1 is the right 1st root of the 4th ganglion. The 1st ganglionic roots, containing the majority of mechanoreceptor afferents of the segment, were exposed laterally by removing the overlying longitudinal muscle fibers of the 3rd segment. Most experiments were performed on the right 1st root, 4r1, since this is composed almost entirely of sensory afferents. Two preparations were used: (1) the isolated abdominal nerve cord is composed of abdominal ganglia 2–6. All peripheral nerves were cut, except for 4r1 and 4r3, which contains the axons of the VSM motoneurons. In those experiments in which cutaneous activation of the motoneurons by mechanoreceptors was not desired, 4r1 was cut distally and drawn into a suction electrode for electrical stimulation. In the majority of experiments, 4r3 was cut distally as well and potentials recorded with suction electrodes. (2) The 4th ganglion was isolated by severing the 3–4 and 4–5 connectives close to the 3rd and 5th ganglia. The recording and stimulation procedures were the same as in (1). The preparations were maintained 12.5°C in Cole's solution (in mmol l^{-1}): NaCl 460, KCl 15.7, $CaCl_2$ 25.9, $MgCl_2{\cdot}6H_2O$ 8.3, Na_2SO_4 8.4, buffered with 10 mM HEPES to pH 7.4. A high-Ca^{2+}/Mg^{2+} saline was used in some experiments: NaCl 408.7, KCl 15.7, $CaCl_2$ 64.75, $MgCl_2{\cdot}6H_2O$ 20.75, Na_2SO_4 8.4.

Extracellular potentials from the nerves were recorded either with glass or polyethylene suction electrodes. Signals were amplified with an A-M Systems differential a.c. amplifier with a passband of 10 Hz to 1 kHz and digitized at 5 kHz using a Data Translation DT3831 I/O board. Intracellular recordings from motoneurons were made with 40-MΩ glass pipettes, filled with 2 mol l^{-1} potassium acetate, connected to an Axoclamp 2B amplifier. The 4th abdominal ganglion, from which all intracellular recordings were made, was mechanically desheathed. Two criteria were used to confirm the identity of motoneurons recorded intracellularly: (1) action potentials in the intracellular record were correlated 1:1 with one of the extracellular action potentials in 4r3, and (2) antidromic stimulation of 4r3 produced a short latency intracellular action potential that followed the electrical stimulus to 100 pulses per second (pps) without changes in the latency of the action potential. Intracellular recordings from muscle fibers used 'floating electrodes' (Chapple 1993) in which the tip of a conventional micropipette is suspended from a silver wire. A servo-controlled stimulator was used to displace the cuticle and was controlled by a computer program. The servo-controlled system was composed of a loudspeaker, the amplitude of movement of which was measured with a linear diode (UDT LSC/5D, UDT Sensors, Hawthorne, Calif., USA) excited by an infrared LED mounted on the cone of the loudspeaker. The length signal was sent to a PID controller and then to a power operational amplifier (Burr-Brown 3573AM) that drove the loudspeaker. Ramp signals were generated by the computer; in some experiments, a Wavetek 188 Sweep/Function Generator was gated by the computer to produce sinusoids of different frequencies. To record forces generated by the longitudinal layer of the VSM, a force transducer was attached to plates glued to the cuticle of the third and fifth right segments. The left VSM and 4l3 were removed and the right VSM and 4r3 were left intact. A similar procedure was used to record the forces generated by the transverse/circular layers of the VSM; the force transducer was attached to plates glued to left and right lateral groove regions but both the left and right fourth third roots were left intact, since damage to either root abolishes the response of the transverse/circular layer muscles.

[1]Individual motoneurons are labeled by indicating first the number of the ganglion in which they reside, secondly, the side of that ganglion, thirdly, the ganglionic root that they exit, and finally, the region of muscle innervated. For example: 4r3m is the motoneuron from the 4th abdominal ganglion, on the right side, that exits the 3rd ganglionic root, and ultimately innervates the medial muscle fibers. 4r3c, 4r3i, 4r3t, 4r3cir, 4r3l are motoneurons of the right side 4th ganglion that innervate the central, inhibitor, transverse, circular, and lateral muscle fibers, respectively

Digitized records of extracellular spike trains and intracellular membrane potentials were displayed in Matlab (The MathWorks, Natick, Mass., USA). A threshold was set visually so that the peak-to-peak amplitudes (maximum positive excursion plus the maximum negative excursion) and spike times (measured from a positive to negative zero crossing) for all spikes above that threshold were recorded in a table. An amplitude histogram of all the spikes for the nerve in an experimental file (typically consisting of ten repetitions) was constructed and the lower and upper boundaries for a desired peak selected to define a single unit. These selected spikes were then displayed with the original record to confirm that the desired spike class had been selected and that it was composed of a discrete group of spikes. Spike frequencies are expressed as pulses per second to distinguish them from stimulus frequencies expressed in Hertz.

The probability spike density function (PSDF) was used to indicate the average response of a unit to repeated presentations of a stimulus. In contrast to the peristimulus time histogram (PSTH), which produces a discrete estimate, the PSDF results in a continuous estimate of the probability of firing (Silverman 1986). It was calculated by convolving the time of each spike with a Gaussian distribution kernel with a fixed standard deviation (50 ms), and then sampling the record at 100 Hz. The PSDF was normalized by dividing the kernel by its integral. Figure 1b shows a comparison between the same set of spike times, produced by ten repetitions of a stimulus, averaged using a PSTH, with a bin width of 10 ms, and the PSDF. To examine the probability of firing over a defined interval of time, rather than at one sample point, the integral of the PSDF was calculated by summing its values between the beginning and end of the interval and dividing by the number of sample points in the internal – 'the averaged PSDF'. Relationships between dependent and independent variables were fit with a linear model, to determine whether they covaried, but this does not imply that the underlying relationship was necessarily linear.

Motoneuron identification by extracellular amplitude

Previous analysis of the firing patterns of the VSM motoneurons used excitatory junction potentials (ejps) in muscle fibers to obtain times of motoneuron action potentials (Chapple 1993, 1997). Many of the muscle fibers in a particular region of the muscle are innervated by a single motoneuron, so that ejp and action potential time were obtained using a simple trigger circuit. In the present experiments, it was desirable to insure that, during reflex activation of the motoneurons, feedback of muscle force was not re-exciting the sensory receptors; the nerve containing the motoneuron axons was cut distal to the electrode and the extracellular amplitudes of motoneuron action potentials were used to identify them and record the time of their occurrence. Experiments were performed to match motoneuron ejps in the VSM with their extracellular amplitudes in the right third root of the 4th ganglion, 4r3.

Figure 1 shows the results from an experiment in which a microelectrode was placed in muscle fibers in different regions of the VSM and extracellular potentials from 4r3 recorded with a suction electrode. Figure 1A shows an amplitude histogram of the extracellular potentials of all of the six motoneurons in the 4th right 3rd root, scaled to the amplitude of the smallest spike. Figure 1B shows a recording from the medial motoneuron, 4r3m, (peak 5 in Fig. 1A), one of the two motoneurons that is tonically active (for 4r3m at about 3 pps). Figure 1C shows a recording from the central muscle region on the right side of the 4th segment. The central excitatory motoneuron, 4r3c, (peak 1 in Fig. 1A) has a small amplitude extracellular potential and is the second motoneuron that is tonically active, firing at about 6 pps. Firing intermittently is the inhibitor, 4r3i, (peak 2 in Fig. 1A) with an amplitude in the same range as 4r3c. Figure 1D shows a recording from the lateral motoneuron, 4r3l, (peak 6 in Fig. 1A) a phasic unit that generates a large ejp with an active response; it generates a twitch in the muscle cells it innervates and has the largest extracellular action potential of units within the 4th right 3rd root. Figure 1E shows a recording from a muscle fiber along the margin of the VSM where the circular

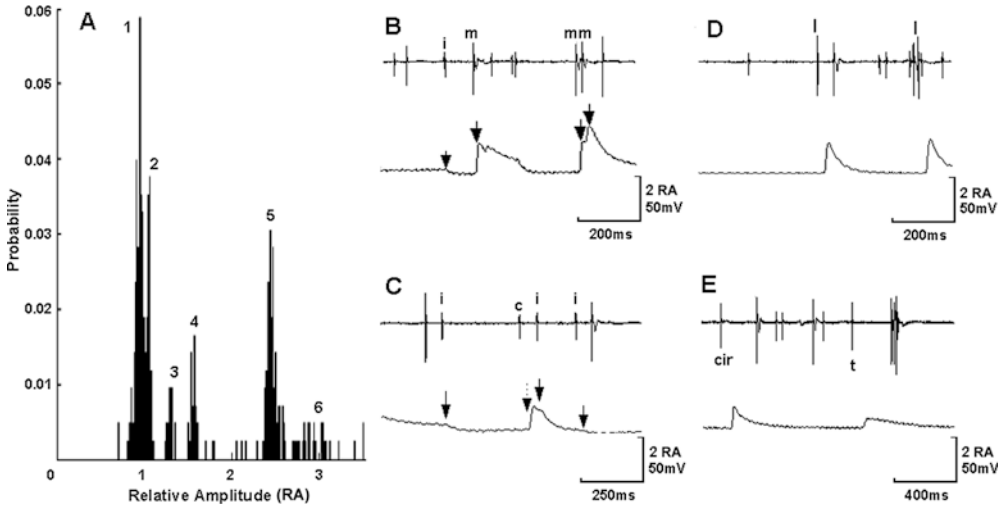

Fig. 1A–E Correlation of the extracellular amplitudes of 4r3 action potentials with excitatory junction potentials (ejps) recorded from different regions of the 4th right ventral superficial muscles (VSM). **A** Extracellular amplitude histogram of 4r3 motoneuron action potentials normalized to the amplitude of the smallest amplitude spike: peak 1. Peak 1 is 4r3c, which innervates the central muscle fibers; peak 2 is the inhibitor, 4r3i; peak 3 is the motoneuron that innervates the circular layer, 4r3cir; peak 4 is 4r3t, which innervates the transverse muscles; peak 5 is 4r3m, the motoneuron that innervates the medial muscle fibers; peak 6 is 4r3l, the motoneuron that innervates the spiking lateral muscle fibers. **B** *Top*: extracellular recording from the motor root of the fourth ganglion (4r3); *bottom*: intracellular (IC) electrode in 4r3m region of VSM. **C** *Top*: 4r3; *bottom*: IC electrode in 4r3c region of VSM. **D** *Top*: 4r3; *bottom*: IC electrode in 4r3l region of VSM. **E** *Top*: 4r3; *bottom*: IC electrode in the transverse/circular layer of VSM. *c* 4r3central, *i* 4r3inhibitor, *c* 4r3circular, *t* 4r3transverse, *m* 4r3medial, *l* 4r3lateral

Table 1 Extracellular amplitudes of the motoneurons scaled to the amplitude of 4r3c

Experiment	4r3c	4r3i	4r3t	4r3m	4r3l
1	1		1.57	3.21	4.44
2	1	1.12	1.53	2.63	3.1
3	1		1.91	4.4	2.8
4	1		1.25	1.8	2.75
5	1		1.61	2.12	3.68
6	1		1.34	3.06	4.17
7	1		1.43	3.77	4.68
8	1		2.0	3.74	4.8
Mean ± SD			1.58 ± 0.26	3.09 ± 0.88	3.8 ± 0.84

and transverse muscles are exposed. Two classes of ejps are observed, each correlated with a different amplitude extracellular action potential (peaks 3 and 4 in Fig. 1A).

The relative amplitudes of the individual motoneurons were similar in different animals. Table 1 shows the results of eight experiments, in which the extracellular amplitudes of the motoneurons, identified by the region of muscle innervated, their tonic frequency and the size of the ejp, were scaled to the amplitude of 4r3c. In the many experiments in which the ejp was not simultaneously recorded with the extracellular signal from 4r3, these relative sizes of the action potentials of the motoneurons were used as one criterion of motoneuron identity.

During an experiment the ratios of extracellular amplitudes were generally a reliable index of motoneuron identity, except during high frequency bursts where there was overlap between extracellular potentials. Although the extracellular amplitudes of the motoneurons were similar in different preparations, they were not always sufficiently distinct to permit an unambiguous identification of a motoneuron. In several preparations, the amplitudes of 4r3m and 4r3l were quite close; in experiment 3 in Table 1 they were actually reversed. Thus, in smaller animals particularly, it was not always possible to distinguish between these two motoneurons. The inhibitor, 4r3i, is normally not active in the isolated abdominal preparation; its amplitude in experiment 2 represents only a single preparation. Thus, it may have been present, but could not be detected, in some preparations in which 4r3 was cut distally. The two motoneurons that innervate the circular and transverse muscle layers of the VSM, 4r3t and 4r3cir (which is not shown since it could not be reliably separated from 4r3t in different preparations) were identified by recording from the lateral margins of the VSM where the circular and transverse layers of muscle insert on the connective tissue of the lateral groove. Attempts to record from these layers in the more ventral regions of the VSM where they are surrounded by several layers of the longitudinally aligned muscle fibers and cuticle were not successful. Thus, it has not been possible to consistently discriminate between them on the basis of the muscle fibers they innervate. Since their amplitudes lie between 4r3m and 4r3c and they fire phasically in response to mechanoreceptor activation, the larger of the two, 4r3t, was used to examine their reflex properties. Thus, although extracellular spike amplitude is a useful criterion of motoneuron identity, it must be supplemented by other criteria. Two of these, the level of tonic firing and the behavior of the motoneurons in response to reflex activation, were used to further identify the motoneurons when the 3rd root was cut distal to the electrode. In isolated abdominal preparations, only 4r3c and 4r3m fire tonically, 4r3m at a frequency about one third that of 4r3c. 4r3l is normally not active and 4r3t and 4r3cir fire at low intermittent frequencies. 4r3l, 4r3t and 4r3cir are phasically activated by mechanoreceptor stimulation in the isolated abdomen. Thus, in these experiments, extracellular amplitude, tonic frequency and the response to reflex activation were all used as criteria for identifying the motoneurons.

Results

Reflex response to cutaneous stimulation

Deflection of the cuticle evokes a characteristic response in each motoneuron (Fig. 2A). The PSDF was used to analyze motoneuron response over a minimum of ten repetitions of a deflection of the cuticle of the abdomen. The medial motoneuron, 4r3m, exhibited an initial high

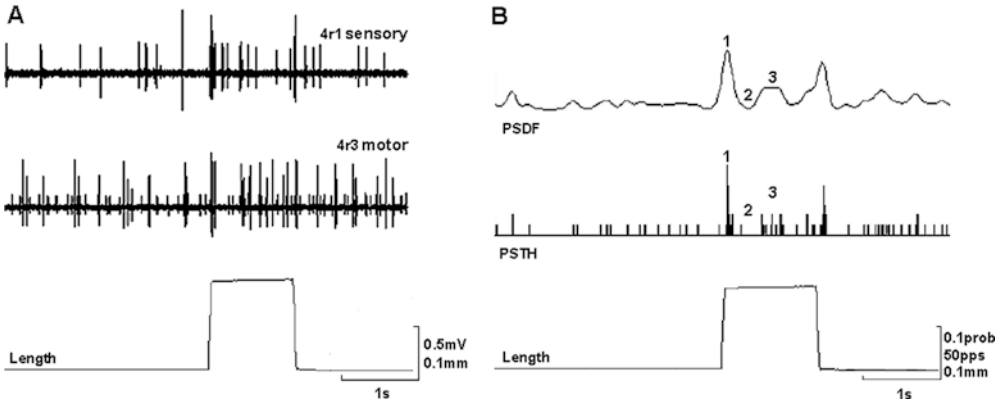

Fig. 2A, B Reflex activation of VSM motoneurons by cuticular displacement. **A** *Top trace*: sensory units in 4r1; *middle trace*: motoneurons of 4r3. At the onset of displacement (*bottom trace*) both sensory and motoneurons are activated, but there is a brief pause in the frequency of the motoneurons followed by an increased period of firing. **B** The averaged response ($n = 10$) for one motoneuron, 4r3m, is displayed as a probability spike density function (PSDF, *top*) and a peristimulus time histogram (PSTH), bin width 0.01 s (*middle*). The PSDF provides a continuous estimate of the average probability of firing of a single unit. The three phases of the tri-phasic reflex are noted on both the PSDF and PSTH traces

frequency peak beginning about 80 ms after the displacement of the cuticle and lasting for 100 to 180 ms (Fig. 2B, phase 1). This was followed by a period of lowered probability of spiking (phase 2), with a peak latency of 250 ms and a duration of 160 to 200 ms. Finally, phase 2 was followed by a period of elevated probability of firing (phase 3) with a latency of 400 ms lasting for a variable duration between one and a few seconds (Fig. 2A, middle). The small tonic central unit, 4r3c (Fig. 3C), exhibited a prominent and transient decrease in its tonic firing rate in frequency and probability of firing lasting for 180 ms, with a latency of the peak of the reduction in probability of 200 ms, followed by an increase in probability (latency of 450 ms) lasting for about a second. In some preparations, 4r3c showed an initial peak before the decrease in frequency. 4r3l and 4r3t (Fig. 3C) were usually not tonically active in the isolated abdomen and showed single PSDF peaks, similar in amplitude, duration and latency to the initial peak in 4r3m. In some preparations where 4r3l and 4r3t showed higher tonic frequency, there was a period of low frequency firing following the initial burst and then a period of increased excitation.

In contrast to the motoneurons, touch evoked a single phasic burst in the mechanoreceptors. One amplitude

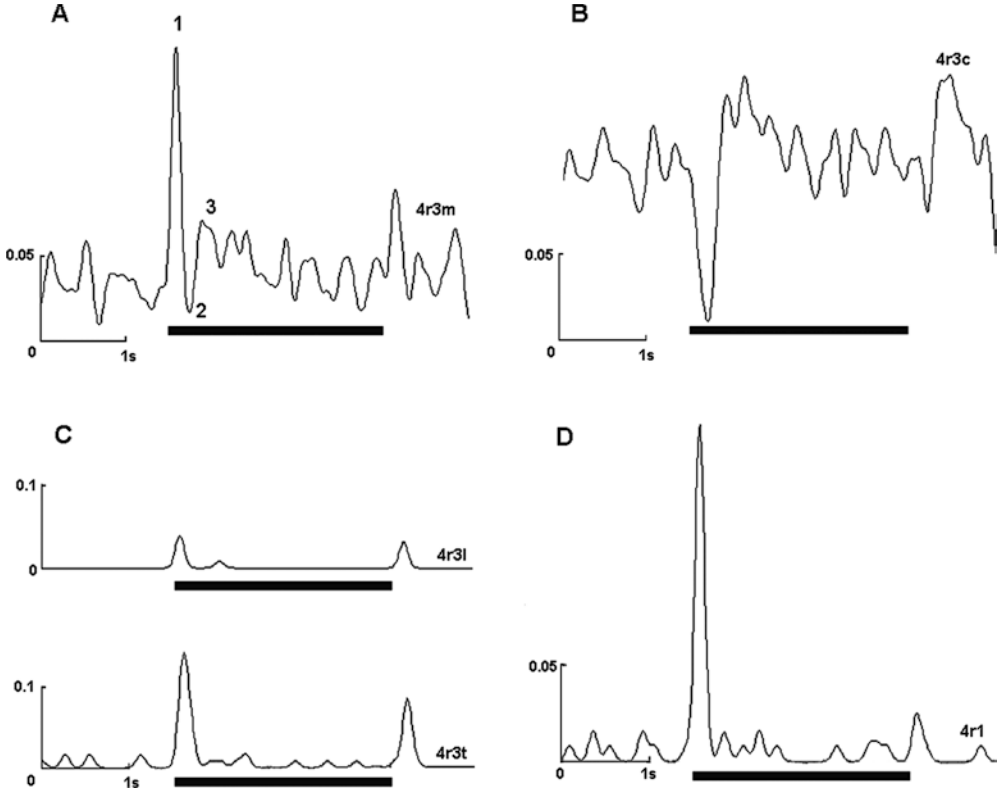

Fig. 3A–D Averaged PSDF reflex responses of identified motoneurons to cuticular displacement. *Dark bar* beneath the plot indicates the duration of cuticular displacement. **A** 4r3m, (*1*) initial burst, (*2*) brief inhibition and (*3*) increased probability of firing. **B** 4r3c, initial inhibition followed by increased probability of firing. **C** *Top*: 4r3l; *bottom*: 4r3t, both with phasic burst at the onset and offset of stimulation. **D** 4r1, single amplitude class of a mechanoreceptor with a phasic burst at the onset and offset of displacement. Vertical axes represent probability—from the PSDF—per sample period (10 ms)

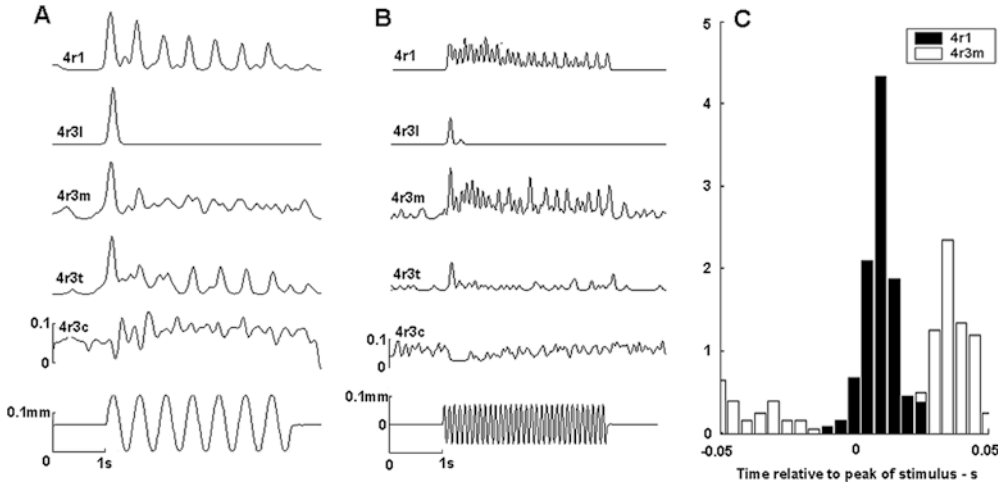

Fig. 4A–C Reflex activation of motoneurons, shown as PSDFs, by sinusoidal deflection of the cuticle. **A** 2 Hz frequency (*bottom trace*). The initial high probability of firing decreases to a steady-state level in two of the motoneurons, 4r3m and 4r3t, with a progressive adaptation that is also present in the inhibitory component of the response 4r3c. **B** 10 Hz frequency, sampling interval 5 ms, standard deviation of Gaussian in PSDF is 25 ms. At this frequency there is a pronounced adaptation in the motoneurons 4r3l and 4r3t as well as the inhibition of 4r3c. **C** Phase histogram of one sensory afferent in 4r1 and the initial peak of 4r3m, showing that this component can follow displacement to at least 10 Hz. In **A** and **B**, vertical axes represent probability per sample period, except in the bottom traces

class of mechanoreceptor is shown in Fig. 3D. This afferent did not exhibit a period of decreased frequency and was not followed by a secondary increase in frequency. Placing the nerve cord in a high-Ca^{2+}, high-Mg^{2+}, reduced-Na^{+} saline, which reduces the activity of polysynaptic pathways (Berry and Pentreath 1976), abolished the late excitatory phase in the reflex response, as well as the tonic firing of all motoneurons. These were restored upon returning the nerve cord to normal saline. In preparations in which the 4th ganglion was not isolated from the rest of the abdominal nervous system, mechanical stimulation of the cuticle as well as electrical stimulation of 4r1 would often evoke an additional long (several seconds), variable latency activation of the motoneurons with an irregular duration and frequency of firing. This was often separate from the initial pattern of activation.

Repeated stimulation of the cuticle, using a sinusoidal stimulus, produced a motoneuron burst for each cycle in some of the motoneurons, as well as an overall elevation in tonic frequency. Figure 4A shows the averaged response to a 2-Hz sine wave in a single amplitude class of sensory receptor in 4r1 and in 4r3l, 4r3m, 4r3t and 4r3c. Peak values of probability of firing for 4r3m and 4r3t motoneurons were correlated with the sensory peaks and the decrease in firing of 4r3c occurred at the same latency as in the case of a single stimulus. 4r3l rapidly adapted to the stimulus. The reduction in the peak response of the motoneurons after the first cycle was correlated with the reduction in the mechanoreceptor, suggesting that there is a close association between sensory and the motoneuron response and that much of the adaptation may be occurring peripherally. At 10 Hz (Fig. 4B) both 4r3l and 4r3t rapidly adapted, 4r3m showed a sustained elevation in the probability of firing and 4r3c showed a pronounced inhibition that decreases and thus is followed by a period of increased probability of firing. The plot of sensory and 4r3m spike times relative to the peak of the sinewave stimulus shows a sharp peak with a latency of 28 ms from the peak of the 4r1 response to the peak of 4r3m (Fig. 4C). Inhibition and late excitation were obscured by the initial burst of the subsequent stimulus. Although peaks were observed in the cyclogram when stimulating at 20 Hz (not shown), there was overlap between the first two phases of the reflex response. Successive stimuli are separated by 50 ms, much less than the latency of the reflex.

This alternation between an initial burst, a sharp reduction in spike frequency and a subsequent modest elevation in frequency could be due to the activation of different central neurons by the mechanoreceptors. Two other possibilities are that this pattern of activation is generated by fast and slow conducting populations of sensory fibers activating the motoneurons at different times or by mechanical coupling between muscles and sensory fibers in parallel, as is observed in the 'silent period' of muscle spindles. This question was examined by isolating the abdominal central nervous system and inserting an intracellular electrode into a motoneuron. In Fig. 5A, touch to the cuticle produced a pattern of depolarization of 4r3m from which several spikes arose, often reaching instantaneous frequencies of 250 pps, followed by a pause in firing and a hyperpolarization of the motoneuron generated by a complex burst of post-synaptic potentials (psps), many of which appear to be ipsps, and then a subsequent increase in epsps frequency from which action potentials were initiated. Even during high-frequency firing of mechanoreceptor afferents, 4r3m did not fire long trains of spikes. Figure 5B shows the activation of 4r3m by a single electrical stimulus to the sensory nerve cut distal to the electrode.

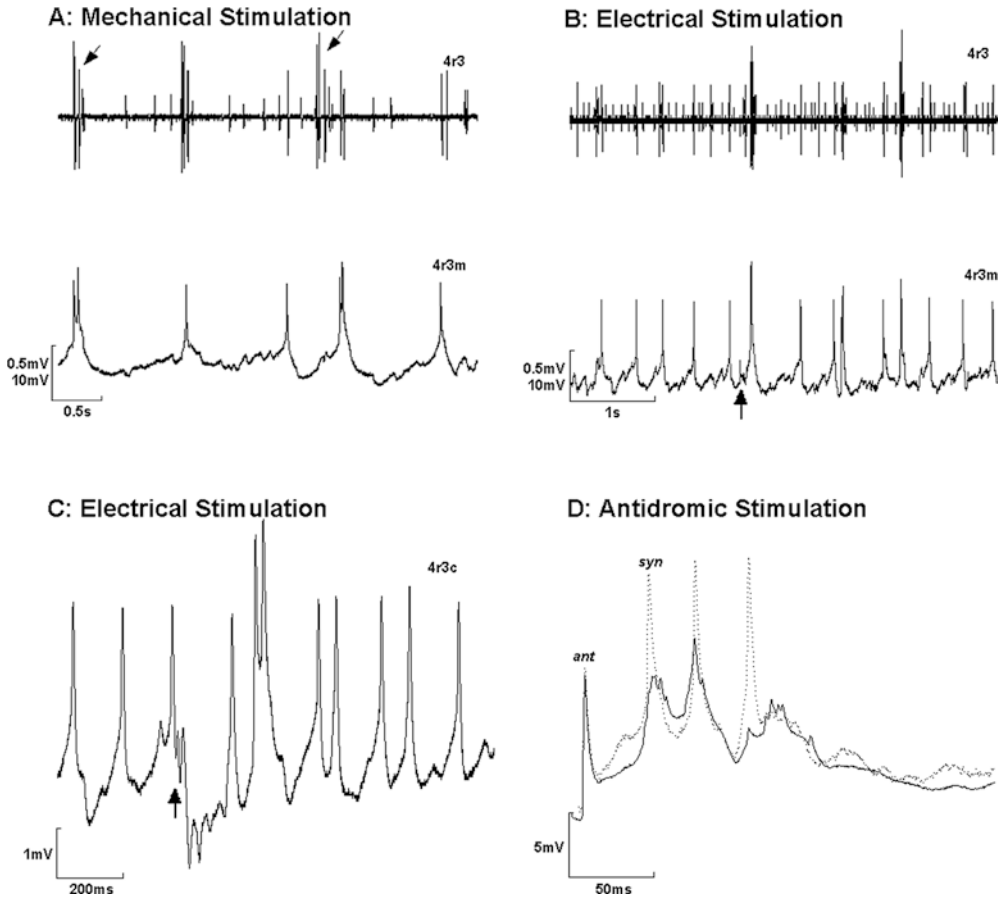

Fig. 5A–D Intracellular recording of membrane potentials in the postural motoneurons. These traces illustrate the synaptic potentials underlying the reflex response. **A** Mechanical stimulation (*arrows*) of the left superficial dorsal muscle (DSM). Following the reflex burst there is a hyperpolarization composed of inhibitory post-synaptic potentials (ipsps) followed by a period of late excitation with excitatory post-synaptic potentials (epsps) and ipsps. **B** Electrical stimulation (*arrow*) of the sensory root, 4r1, in the isolated abdominal nerve cord; distance between the 4th ganglion and stimulating electrode of 25 mm. After the initial burst, which in this example is a single spike, there is a period of hyperpolarization in which small ipsps are present. Following this is a combination of ipsps and epsps, from which spikes arise at a higher frequency and variability than those preceding stimulus. **C** Electrical stimulation (*arrow*) of 4r1 while recording from the motoneuron innervating the central muscles, 4r3c. There is a pronounced hyperpolarization produced by ipsps followed by an excitatory period during which spikes arise from compound epsps. **D** Antidromic stimulation of the motor root, 4r3, while recording intracellularly from one motoneuron, 4r3m. *Solid line* is the averaged intracellular record from 10 trials; the *dotted line* is the record from a single trial: *ant* antidromic spike, *syn* synaptic spikes; the stimulus artifact was set to starting time point in the figure. There is no indication of an inhibitory period following the reflex burst in response to antidromic stimulation

The initial burst of action potentials arises from a group of short-latency epsps. In one experiment, the conduction velocity of a single sensory afferent at threshold was 0.46 ± 0.03 m s^{-1} and the distance between stimulating electrode and the perimeter of the ganglion was 6.9 mm; the latency between stimulus onset and initial epsp was 17.1 ± 1.3 ms ($n = 20$). After accounting for a conduction time of 15 ms, the remainder of 2.1 ms is consistent with a monosynaptic connection between afferent and motoneuron. In three other experiments, synaptic latencies of the same order were recorded. The following period, phase two, contained a number of ipsps that hyperpolarized the membrane potential below the tonic firing level. This was followed by a late elevation in motoneuron frequency that arose from a depolarization composed of high frequency indistinct synaptic potentials. The presence of psps following single afferent spikes suggests that they are generated by central interneurons rather than lasting peripheral input. Figure 5C shows an intracellular recording from 4r3c in an isolated 4th ganglion. There is an initial period of inhibition with prominent ipsps, with a minimum latency of 30.0 ± 7.5 ms ($n = 20$), followed by a later period of excitation. In Fig. 5C, the ipsps firing during the period of hyperpolarization are occurring at high frequencies. In some preparations, there was an initial burst of epsps observed before the prominent inhibition in 4r3c. Antidromic stimulation of 4r3 produced a short latency direct spike in 4r3m (Fig. 5d) that followed a train of stimuli to 100 Hz, as well as a longer latency burst of action potentials that arose from synaptic potentials that followed antidromic stimuli to 2 Hz. This pathway did not produce a prominent period of inhibition followed by increased excitation, suggesting that the inhibitory peri-

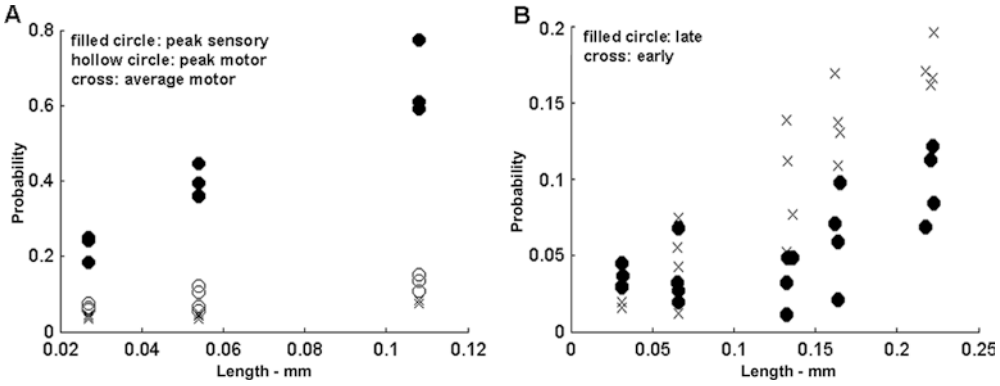

Fig. 6A, B Relation between probe displacement and probability of firing of the motoneuron, 4r3m. **A** Comparison of the maximum peak probability of a single amplitude class of a mechanoreceptor in 4r1 (*solid circles*), the maximum initial peak probability of 4r3m (*open circles*) and the average (*crosses*, from 2.0 to 2.5 s) probability of 4r3m. Both measures of motoneuron probability increase much less than the sensory receptor over the range of displacements. The linear regression equation of 4r1 (maximum probability of firing in 10 ms) = 0.093 + 5.27×step amplitude (mm); $r^2 = 0.91$. The linear regression equation of 4r3m (maximum probability of firing in 10 ms) = 0.045 + 0.80×step amplitude (mm); $r^2 = 0.62$. The average probability of firing/10 ms of 4r3m between 2.0 and 2.5 s = 0.022 + 0.50×step amplitude (mm); $r^2 = 0.85$. **B** Comparison of the rate of increase of 4r3m probability in the first 0.5 s and in 1.0–2.0 s after the onset of probe displacement. The early portion of 4r3m response increases linearly with displacement. The later portion has a constant response up to 0.13 mm and then increases with displacement. The average probability of firing was: 4r3m = −0.0023 + 0.80×step amplitude (mm) ($r^2 = 0.85$, $n = 20$) in the first 0.3 s and, in the interval between 1.0 and 2.0 s after the displacement, the average probability of firing was 0.016 + 0.31×step amplitude (mm) ($r^2 = 0.46$, $n = 20$)

od in Fig. 5A–C is not arising from recurrent collaterals of motoneurons. Intracellular recordings from 4r3l (not shown) also showed an initial burst of epsps and a period of inhibition, followed by increased synaptic potentials during the post-burst period. The initial burst of epsps in both 4r3l and 4r3m followed stimulus frequencies of 4r1 one-to-one to between 10 and 12 pps. Thus, in all three motoneurons activation of sensory receptors produces a short latency group of epsps, followed by longer latency epsps and ipsps generated by interneurons. All of the motoneurons exhibited tonic epsps and ipsps in the absence of sensory stimuli.

Reflex intensity as a function of stimulus intensity

To examine the relationship between displacement of the cuticle and the reflex response, mechanical displacement was used to deflect the surface of the dorsal cuticle of the fourth right segment and the peak of the initial response was examined in a discrete class of sensory amplitudes and in 4r3m. One way that this relationship can be examined is with the analysis of local maxima and minima of PSDFs calculated for trials over which sensory activity was varied. Figure 6A shows the relationship between the peak of a PSDF of a large sensory unit recorded in 4r1, and two measures of the response in 4r3m. Both the peak probability of the initial burst from 4r3m and the average probability increased at about a fifth the rate of the sensory unit. A PSTH (not plotted) was also calculated and fit to a regression relationship: pps = 2.38 + 61.9×step amplitude (mm), $r^2 = 0.86$; showing a similar relationship. Thus, the initial burst in 4r3m covaried with the selected sensory unit as a function of displacement but with a much smaller slope, as estimated by several methods.

The dependence of the later portion of the reflex on displacement was also examined (Fig. 6B). At the smaller amplitudes of displacement the probability of the interval between 1.0 and 2.0 s did not increase (although it was much above the average probability of firing in the second before stimulation: 0.009 ± 0.006), but as the amplitude increased there was a point (0.13 mm.) at which the late excitatory response in Fig. 6B increased with a slope similar to the initial burst. The average decrease in the probability of firing during the inhibitory period of 4r3c was less correlated with stimulus intensity ($r^2 = 0.28$) and the average probabilities of the late excitatory period in 4r3t ($r^2 = 0.16$) and 4r3c ($r^2 = 0.045$) did not significantly increase with displacement amplitude, although there was a non-significant trend for their average probability of firing to increase slightly with step amplitude. This modest increase in motoneuron probability of firing was observed in all preparations.

Electrical pulses were also used to stimulate sensory axons of 4r1 over a wide range of thresholds. This experiment isolated the ganglion from all peripheral feedback pathways. Single pulses of current were used to electrically stimulate 4r1, cut distal to the stimulating electrode. Although there was generally an increase in the probability of motoneuron firing as stimulus current was increased, there was considerable adaptation in the response so that linear regressions were not significant over a range of one to five times threshold current. Stimulus trains with equal numbers of current pulses delivered at different frequencies did not show a significant relationship between peak initial probability of motoneuron firing ($r^2 = 0.099$), average initial probability ($r^2 = 0.0058$) or average late probability ($r^2 = 0.27$) although the peak force produced by the muscle under these conditions was significant ($r^2 = 0.85$, $P < 0.027$).

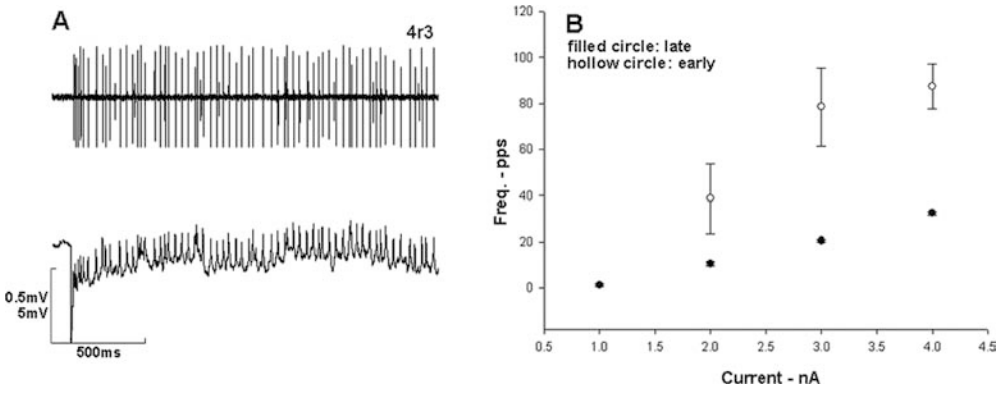

Fig. 7A, B Activation of the motoneuron, 4r3m, by intracellular depolarization. **A** A 4-nA depolarizing current produces an initial period of higher-frequency spikes followed by a lower-frequency sustained train that shows little adaptation. **B** Plot of current versus frequency for the first 5 spikes (*open circles*) and for the subsequent train (*filled circles*). Error bars are standard deviations, $n = 10$

The modest response of the motoneurons to both mechanical and electrical activation via 4r1 does not appear to arise from intrinsic membrane properties. The motoneurons are capable of sustained firing over a much greater range of frequencies than those observed during reflex activation. Figure 7A shows an experiment in which 4 nA of current passed through a microelectrode elicited increased tonic firing in 4r3m. At the onset of stimulation there was a period of higher frequency firing lasting for about 100 ms, after which the frequency decreased to a relatively constant level that lasted for the duration of stimulation. Figure 7B shows a current-frequency plot of the first five spikes and for the subsequent 1.9 seconds for ten repetitions at each current. The frequency of the first five spikes doubles from 2 to 3 nA but shows much less increase from 3 to 4 nA. In contrast, the frequency of the following 1.9 s shows a more gradual but linear slope over the entire range of applied currents, with a slope of about 10 pps nA^{-1}. During the later portions of the response to current, there was no adaptation of the frequency of 4r3m.

VSM forces

Reflex activation of the motoneurons produced an increase in force, lasting for several seconds, of both the longitudinal and transverse/circular layers of the VSM. Measurements of the time to peak for the two muscle layers were slightly different. A single electrical stimulus produced forces reaching their peak in 0.289 ± 0.107 s ($n = 10$) in the longitudinal layer and 0.535 ± 0.059 s ($n = 10$) for the transverse/circular layer. The minimum time constants for decay from peak tension were 1.6 ± 0.51 s for the longitudinal layer and 1.25 ± 0.6 s for the transverse/circular layer. These values did not significantly vary with stimulus intensity above 1.25 times threshold but did vary between preparations. The transverse/circular layer produced a greater maximum reflex force than that of the longitudinal layer. This was not the result of differences in reflex activation since direct stimulation of the motoneuron axons by stimulating 4r3 showed a similar ratio of forces. Length-tension measurements of the two layers, in animals of similar size, had peak forces at the optimum length of 2.18 ± 0.02 N for the transverse/circular layer and 0.55 ± 0.01 N for the longitudinal layer. The peak of the transverse/circular length-tension relationship was three times broader than that of the longitudinal layer.

The magnitudes of forces produced by reflex activation of the two layers of the VSM are much smaller than those produced by direct activation of the motoneuron axons. Figure 8A shows the reflex activation of the longitudinal layer by a step displacement of the cuticle. This produced a peak force of 0.064 N, a force of the same order of magnitude as produced by electrical stimulation of 4r1. Similar to the results obtained with the estimates of the probability of firing, electrical stimulation of the sensory nerve using either single stimuli of different magnitudes above threshold or trains of stimuli did not produce systematic increases in force with stimulus intensity. This appears to be due, in part, to a habituation of the reflex, since the first few trials of a series often produced greater forces than those at the end of the series of repetitions. Increasing stimulus frequency, as mentioned above, did significantly increase muscle force. Figure 8B shows three trials from different series, two stimulating the sensory nerve to evoke the reflex: a 0.2-s train at 40 Hz, and a 1.6-s train at 40 Hz, and one train stimulating the motoneuron axons at 60 Hz for 2.0 s to maximally excite the muscle directly. The time constant for the decay of the short train was 1.33 ± 0.14 s ($n = 10$). The longer duration train resulted in an elevation in force that considerably outlasted the period of stimulation and was due to the elevation in tonic frequency of the motoneurons. When the peak reflex force from many trials of different stimulus conditions was divided by the peak force of the muscle produced by direct stimulation of 4r3 to produce a histogram of the distribution of reflex force, means of 0.25 ± 0.09 ($n = 100$) and 0.08 ± 0.02 ($n = 80$) were obtained for the longitudinal layer and means of 0.15 ± 0.07 ($n = 90$) and 0.21 ± 0.04 ($n = 50$) for the transverse/circular layers (four animals). The histogram of a fifth experiment is plotted in Fig. 8C. Its mean was 0.083 ± 0.015 ($n = 80$). These were in the same range as those forces elicited by touch to the cuticle. In addition, the peak probabilities of 4r3m were calculated in these experiments; these were in the same range of values

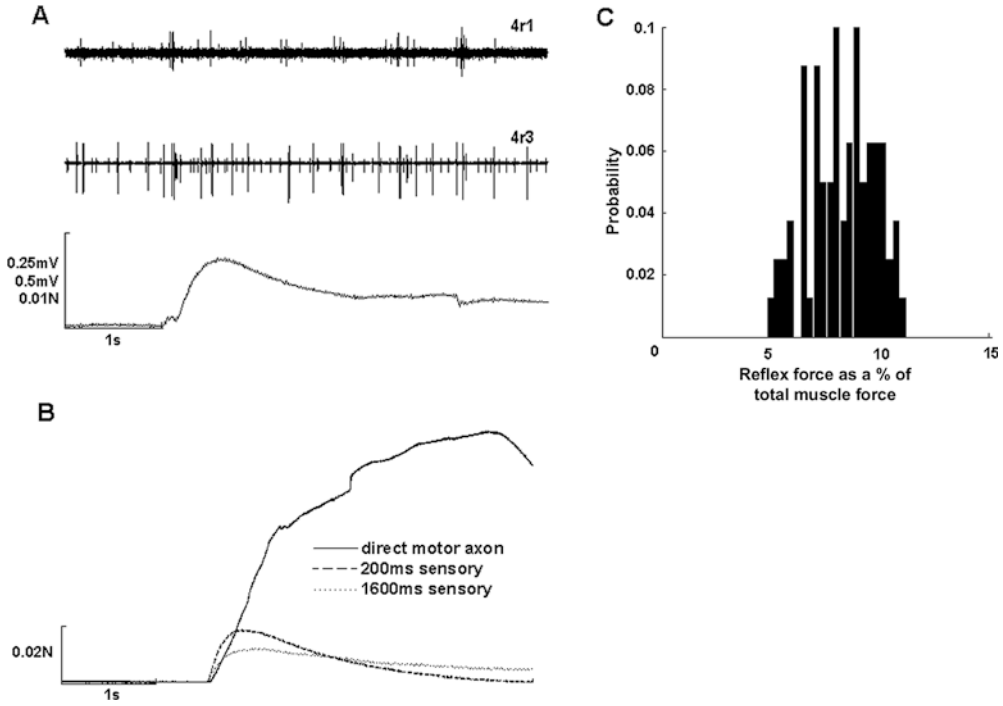

Fig. 8A–C Force in VSM muscle produced by reflex activation of the motoneurons. The force produced by the reflex is much smaller than the maximum force that the muscle can generate. **A** Step deflection of cuticle produces a peak force 6.4 mN. *Top trace* is the sensory nerve, 4r1, *middle trace* the motor nerve, 4r3, and the *bottom trace* the force of the right 4th segment longitudinal layer of the VSM. Irregularities in the force trace arise from mechanical transients of the stimulus. **B** Electrical stimulation of 4r1 with two 40-Hz trains, one lasting for 0.2 s and the other for 1.6 s. Direct stimulation of the motoneuron axons in 4r3 at 60 Hz for 3 s produces a much greater contraction. The irregularities on the direct trace are due to a shifting in the position of the plate holding the transverse/circular layer of muscle. **C** Histogram of the percentage of maximum possible muscle force (see direct stimulation **B**) recruited through reflex activation. This value is computed by dividing the force generated during the reflex by the peak force produced by direct stimulation of the motor root, 4r3, at 60 Hz for 3 s. These experiments were performed while recording force generated by the longitudinal layer of the right VSM. Peak amplitudes of reflex force are nearly an order of magnitude smaller than the forces produced by direct activation of the muscle. Train stimuli of varying durations ($n = 80$)

as observed during experiments in which a step was applied to the cuticle or electrical stimuli applied to 4r1. Thus, reflex activation of the VSM motoneurons by afferents of 4r1 in the isolated abdominal nervous system produced only a fraction of the total force of which the muscle is capable.

Spatial independence of reflex activation of motoneurons

Stimulation of different regions of the fourth segment with a constant amplitude deflection of the cuticle did not show any significant variation with the spatial location of the probe in the pattern of motoneuron response; 4r3m showed an initial burst, a period of inhibition and the subsequent increase in frequency in response to displacement of the cuticle at all regions in the segment. The average probability of 4r3m during the first 300 ms after the deflection with ten repetitions at each of 14 sites around the circumference of the segment was compared using a single-factor ANOVA; the differences were not significant at the 5% level ($P < 0.084$). In another experiment, the probe was shifted between left and right sides, so that afferents in 4l1 or 4r1 activated the motoneurons. In this case as well there was no significant difference in the activation of 4r3m (t-test, $P < 0.37$). When the probe was moved along the longitudinal axis, from the caudal margin of the right 4th pleuron to the rostral margin of the right 5th pleuron, reflex activation of the motoneurons did not appear to differ significantly between different regions but this relationship was not measured quantitatively. In addition, 4r3m was also activated by stimulating the sensory nerves of other abdominal ganglia, using single electrical stimuli (2r1, 3r1, 5r1, and nerves of the 6th ganglion, data not shown). Thus, afferents from all regions of the abdomen reflexly excite 4th ganglion motoneurons.

Discussion

Activation of the postural muscles of the isolated hermit crab abdomen by cuticular mechanoreceptors is generated by monosynaptic activation of the motoneurons followed by periods of inhibition and excitation that are generated by interneurons. It is a spatially distributed reflex that does not vary significantly with the site of stimulation on the cuticle and produces an increment in muscle force that is a small fraction of the total force of which the muscle is capable. Although the response of

the motoneurons may be different in the intact animal in which descending pathways may modulate different components of the circuit, previous experiments with EMG recordings from these muscles suggest that qualitatively the responses are similar in intact animal and isolated abdominal preparations.

The present experiments as well as previous results appear to rule out any continuous feedback model for the control of abdominal position or stiffness. The configuration of the abdomen initially suggested that activation of the VSM would generate an upward force on the columella of the shell, lifting it and rotating it to the left. At the same time, antagonist muscles such as the transverse/circular VSM and the DSM would be inhibited, as occurs in the homologous muscles in macrurans. However, what actually occurs is a co-activation of all of the postural muscles of the abdomen to movement in any direction. Moreover, this co-activation is triggered by mechanoreceptors from the entire abdominal surface. There are mechanisms in the hermit crab nervous system for generating a reciprocal activation of the VSM and DSM; when the animal enters a new shell the abdomen is straightened and extended, due probably to the inhibition of the longitudinal VSM and the excitation of DSM and transverse/circular VSM. Thus, this co-activation is a reflex response to cuticular strain and not an invariant feature of motoneuron activation.

A second feature of the response is that motoneuron activation outlasts the response to a single stimulus; cuticular displacement produces an initial monosynaptic response followed by a sequence of centrally generated inhibition and excitation. The probability of firing of individual motoneurons as well as the total force in the muscle does not vary greatly with stimulus intensity; most stimuli produce a relatively discrete elevation in muscle force and stiffness. A train of electrical stimuli to the sensory nerve increases the duration of the response but does not substantially increase muscle force, in contrast to direct stimulation of the motor nerve. This suggests that central mechanisms may be acting to limit the magnitude of the response. Since intracellular recordings from the motoneurons show epsps and ipsps during tonic firing as well as epsps and ipsps associated with the different components of the response, it is likely that these central mechanisms include excitatory and inhibitory interneurons that act on the motoneurons.

Although feed forward activation of the mechanoreceptors increases muscle stiffness, its operation in the intact animal is not clear. One possibility is that the reflex is a mechanism for correcting for larger displacement of the shell by transient forces that cannot be corrected for by the resting abdominal tone. One difficulty with this is that the latency of the reflex is quite long—of the order of 300–400 ms to peak force. Preliminary measurements of the frequency of oscillation of a shell in water in response to displacement give values of about 1 Hz, a time constant of 160 ms. The existence of a period of elevated motoneuron firing frequency after the initial burst suggests that the reflex is not simply increasing stiffness for a brief period after mechanoreceptor activation, but over a longer period of time as well. A second possibility is that the mechanoreceptors activate the motoneurons by small aperiodic bursts arising both from forces generated by the movement of the shell against the cuticle and from movement of fluid inside and outside of the shell. The mechanoreceptors have low thresholds to low-frequency disturbances (Chapple 2002). They activate VSM motoneurons to fire in a bursty fashion with an interspike interval histogram composed of a short interval component that is abolished when the sensory nerve is cut as well as a longer interval component (Chapple 1997). The two mechanisms are not mutually exclusive; larger displacements of the shell might be preceded by turbulence that would be resisted by the tonic stiffness of VSM muscle. However, the hypothesis that tonic stiffness is produced by stochastic firing of the motoneurons and that afferent signals are integrated to restrict tonic firing within limits might explain the stable level of resting force. A prediction from this model would be a correlation between the tonic firing statistics of the motoneurons and turbulence in the surrounding medium; there would not be a discrete change in the autocorrelogram distribution as the amplitude of external noise is increased.

These observations suggest that the mechanical properties of the VSM, particularly its lengthening force-velocity properties are most important in determining the response of the abdomen to disturbances. These properties have been investigated in crustaceans in only a few cases. In fast muscle Josephson (1999) and Josephson and Stokes (1999) showed that strain rates between 0.3 and 0.6 muscle lengths s^{-1} produced a short-range yield with an actual decrease in force, similar to that observed in frog. In the VSM (Chapple 1983), a slow crustacean muscle, only a gradual decrease in the rate of rise of force was observed at strain rates of up to 2.0 muscle lengths s^{-1}; possibly due in part to compliance of the series elastic element. The mechanical time constants for the muscle, using a two exponent model, were 9 and 90 ms. For force levels below 25% of maximum isometric force and stretch velocities below 5 muscle lengths s^{-1} the peak force of the muscle behaves as a linear elastic element, the stiffness of which is controlled by the level of activation (Chapple 1989). Thus, mechanically the VSM could operate to resist disturbances. Since it is a gradedly activated non-spiking muscle the ejps generated by the motoneurons are small at low frequencies and increase in amplitude due to facilitation. Thus, activation kinetics should operate as a bandpass filter with a lower cut-off frequency defined by facilitation kinetics and the velocity sensitivity of the mechanoreceptors and an upper cut-off frequency defined by the maximum degree of activation of the muscle. To maintain tone the mean frequency of the motoneurons would have to exceed the lower cut-off frequency. A stochastic activation of the motoneurons would ensure that the level of facilitation of the moto-

neuron terminals was great enough to maintain muscle tone but not so large as to be energetically expensive.

The behavior of the motoneurons seems to be consistent with these requirements. The high frequency burst observed in 4r3m, 4r3l, and 4r3t would rapidly increase the amplitudes of their ejps, whereas the ejps of 4r3c, which normally fires at a higher frequency, are at their maximum amplitudes and so would require a smaller initial excitatory burst. The second phase of the reflex response, a period of active inhibition generated at least in part by hyperpolarizing potentials, is puzzling. It might limit the rate of increase in muscle force generated by the initial burst. Although it would seem appropriate to activate the inhibitory motoneuron during this phase to reduce the rate of increase of force, extensive search has not identified ijps from the inhibitory motoneuron in any of the VSM regions during this period. It is possible that peripheral inhibition would reduce stiffness too sharply to operate in a modulatory fashion; central inhibition might provide a more graded way of adjusting steady-state muscle force, as was suggested for the velocity dependent inhibition in the coxo-basipodite depressor reflex in crayfish (Le Ray and Cattaert 1997). The third phase of the reflex response, an elevation of the tonic firing of the motoneurons, is probably the major mechanism for maintaining muscle stiffness by the stochastic firing of the mechanoreceptors. It is most prominent in 4r3m and 4r3c, although in some preparations a second period of enhanced firing can also be see in 4r3l and 4r3t. This response can last for a number of seconds. In intracellular recordings from VSM motoneurons, there is a complex series of synaptic potentials that depolarize the motoneurons much less than during the initial burst. The low frequency of motoneuron firing during this period is unlikely to be due to the intrinsic properties of motoneurons, since, after the first 200 ms of current injection, the motoneuron fired at a constant rate for the remaining period of stimulation. As intracellular current increased so did the frequency, and its rate was much greater than that observed during the late phase of reflex excitation, even when excited by long trains of electrical stimulation. Thus, whatever elements are driving the motoneurons during this late phase do not activate them maximally.

Reflex activation of the muscle transiently increases the force in both longitudinal and transverse/circular layers by a small fraction of the total force produced by direct stimulation of the motoneuron axons. This force ranged from 8% to 25% of total force in different preparations; its restricted range appears to be primarily due to the short period of high-frequency firing of the phasic motoneurons during the initial period and the much lower level of activation during the period of late excitation. The difference in total force produced by the two muscle layers is intriguing; its interpretation is complicated by several factors. First, by stimulating 4r3, only one-half of the longitudinal muscle layer but the entire transverse/circular layer was activated. Since the transverse/circular layer of muscle is actually two layers that are oriented approximately 45° to each other it is difficult to tease out the relative contributions of each layer. As the muscle is stretched circumferentially, the transverse layer will contribute an increasing amount to the force generated by the circular layer, so that the relative contributions of different muscle layers to stiffness along one axis requires the measurement of the angle of each muscle layer to the force transducer. It has been known for a number of years (Alexander 1968) that the hoop stresses in a cylinder under hydrostatic pressure are twice those of the longitudinal stresses, so that it is plausible, on biomechanical grounds, that these differences between longitudinal and transverse/circular layers in this hydrostatic system are real.

Stretch and resistance reflexes mediating load compensation have been primarily investigated in animals with rigid endoskeletons or exoskeletons. In the mammalian stretch reflex, rapid positional feedback from autogenic and heterogenic pathways produces an effective stabilization of joint angle during posture (Burkholder and Nichols 2000). In arthropods, less is known about the actual forces generated during posture. In the best-known system, the stick insect femoral-tibia joint reflex (Bässler 1983, 1993) a high gain and non-linear velocity dependence produces a high stiffness that is an adaptation to the predator avoidance behavior of catalepsy. In locust, the reflex control of the same joint has a low gain and velocity dependence (Ebner and Bässler 1978) and positional signals are more important (Field and Burrows 1982; Newland and Kondoh 1997a, 1997b). In the coxo-basal joint in crayfish (Le Ray et al. 1997) reflex activation of the motoneurons is primarily a function of velocity, although positional signals are available from the chordotonal organ of the joint. Thus, in animals with rigid skeletal systems, positional and velocity feedback regulating the balance of excitation between agonist and antagonist muscles seems to be a basic mechanism for postural control. In these cases, stretch of antigravity muscles is opposed by the reflex activation of these muscles, a negative feedback control. In the leech, an animal with a hydrostatic skeleton like that of the hermit crab abdomen, cuticular strain evokes a bending reflex (Lockery and Kristan 1990), which produces a reciprocal activation of dorsal and ventral muscles. The leech can also produce a shortening behavior produced by P cell activation of dorsal and ventral longitudinal muscle motoneurons (Wittenberg and Kristan 1992), but contraction of longitudinal muscles is associated with a radial expansion of several segments. Thus, the hermit crab abdominal reflex is unusual because phasic afferent signals produce a co-contraction of all abdominal muscles that increases stiffness to oppose external force; the reflex does not produce an obvious change in shape of the abdomen.

Acknowledgements We would like to thank Andrew Moiseff for many insightful discussions and helpful comments on the manuscript, and Mark Grabher and Joseph Healy who provided us with animals. This research was supported by NSF grant IBN-9874499.

References

Alexander RM (1968) Animal mechanics. University of Washington Press, Seattle

Bässler U (1983) Neural basis of elementary behavior in stick insects. Springer, Berlin Heidelberg New York

Bässler U (1993) The femur-tibia control system of stick insects—a model system for the study of the neural basis of joint control. Brain Res Rev 18:207–226

Berry MS, Pentreath VW (1976) Criteria for distinguishing between monosynaptic and polysynaptic transmission. Brain Res 105:1–20

Burkholder TJ, Nichols TR (2000) The mechanical action of proprioceptive length feedback in a model of the cat hindlimb. Motor Control 4:201–220

Chapple WD (1973a) Role of the abdomen in the regulation of shell position in the hermit crab, *Pagurus pollicarus*. J Comp Physiol 82:317–332

Chapple WD (1973b) Changes in abdominal motoneuron firing frequency correlated with changes of shell position in the hermit crab, *Pagurus pollicarus*. J Comp Physiol 87:49–64

Chapple WD (1983) Mechanics of a crustacean slow muscle. J Exp Biol 107:367–383

Chapple WD (1985) Reflex control of dynamic muscle stiffness in a slow crustacean muscle. J Neurophysiol 54:403–417

Chapple WD (1989) Mechanics of stretch in activated crustacean slow muscle. II. Dynamic changes in force in response to stretch. J Neurophysiol 62:1006–1017

Chapple WD (1993) Dynamics of reflex cocontraction in hermit crab abdomen: experiments and a systems model. J Neurophysiol 69:1904–1917

Chapple WD (1997) Regulation of muscle stiffness during periodic length changes in the isolated abdomen of the hermit crab. J Neurophysiol 78:1491–1503

Chapple WD (2002) Mechanoreceptors innervating soft cuticle in the abdomen of the hemit crab, *Pagurus pollicarus*. J Comp Physiol A 188:753–766

Cordo PJ, Rymer WZ (1982) Contributions of motor-unit recruitment and rate modulation to compensation for muscle yielding. J Neurophysiol 47:797–809

Dickinson MH, Farley CT, Full RJ, Koehl MAR, Kram R, Lehman S (2000) How animals move: an integrative view. Science 288:100–106

Duysens J, Clarac F, Cruse H (2000) Load-regulating mechanisms in gain and posture: comparative aspects. Physiol Rev 80:83–133

Ebner TJ, Bässler U (1978) Zur Regelung der Stellung des Femur-Tibia-Gelenkes im Mesothorax der Wanderheuschrecke *Schistocerca gregaria*. Biol Cybern 29:83–96

Feldman AG (1980) Superposition of motor programs. I. Rhythmic forearm movements in man. Neuroscience 5:81–90

Field LH, Burrows M (1982) Reflex effects of the femoral chordotonal organ upon leg motor neurons of the locust. J Exp Biol 101:265–285

Full RJ, Koditschek DE (1999) Templates and anchors: neuromechanical hypotheses of legged locomotion on land. J Exp Biol 202:3325–3332

Horak FB, MacPherson JM (1996) Postural orientation and equilibrium. In: Rowell LB, Shepherd JT (eds) Handbook of physiology. Oxford University Press, Oxford, UK, pp 255–292

Houk JC, Rymer WZ (1981) Neural control of muscle length and tension. In: Brooks VB (eds) Handbook of physiology, sect 1. The nervous system. American Physiological Society, Bethesda, MD, pp 257–323

Josephson RK (1999) Dissecting muscle power output. J Exp Biol 202:3369–3375

Josephson RK, Stokes DR (1999) The force-velocity properties of a crustacean muscle during lengthening. J Exp Biol 202:593–607

Le Ray D, Cattaert D (1997) Neural mechanisms of reflex reversal in coxo-basipodite depressor motor neurons of the crayfish. J Neurophysiol 77:1963–1978

Le Ray D, Clarac F, Cattaert D (1997) Functional analysis of the sensory motor pathway of resistance reflex in crayfish. I. Multisensory coding and motor neuron monosynaptic responses. J Neurophysiol 78:3133–3143

Lockery SR, Kristan WB (1990) Distributed processing of sensory information in the leech. I. Input-output relations of the local bending reflex. J Neurosci 10:1811–1815

Newland PI, Kondoh Y (1997a) Dynamics of neurons controlling movements of a locust hind leg. II. Flexor tibiae motor neurons. J Neurophysiol 77:1731–1746

Newland PL, Kondoh Y (1997b) Dynamics of neurons controlling movements of a locust hind leg. III. Extensor tibiae motor neurons. J Neurophysiol 77:3297–3310

Nichols TR, Houk JC (1976) The improvement in linearity and the regulation of stiffness that results from the action of the stretch reflex. J Neurophysiol 39:119–142

Nichols TR, Cope TC, Abelew TA (1999) Rapid spinal mechanisms of motor coordination. Exerc Sport Sci Rev 27:255–284

Prochazka A (1996) Proprioceptive feedback and movement regulation. In: Rowell L, Sheperd JT (eds) Handbook of physiology: exercise, regulation and integration of multiple systems. American Physiological Society, New York, pp 89–127

Roberts TDM (1967) Neurophysiology of postural mechanisms. Plenum Press, New York

Silverman BW (1986) Density estimation for statistics and data analysis. Chapman and Hall, London

Wittenberg G, Kristan WB (1992) Analysis and modeling of the multisegmental coordination of shortening behavior in the medicinal leech. I. Motor output pattern. J Neurophysiol 68:1683–1692